Journal of JSEM, Vol.7, Special Issue (2007) 114-119

ELECTROCHEMICAL RANDOM SIGNAL ANALYSIS DURING GALVANIC CORROSION OF ANODIZED ALUMINUM ALLOY

Masatoshi SAKAIRI and Yukiya SHIMOYAMA

Graduate School of Engineering, Hokkaido University, Sapporo 060-8628, Japan

ABSTRACT

A new type of electrochemical random signal analysis technique was applied to galvanic corrosion of anodic oxide films formed on 6061-T6 aluminum alloy in NaCl containing 0.5 kmol/m^3 H_3BO_4 / 0.05 kmol/m^3 $Na_2B_4O_7$ solutions. The effect of the anodic oxide film structure on the galvanic corrosion resistance was also examined. During incubation (before localized corrosion started), both current and potential change slightly from the initial value. The incubation period of porous type anodic oxide specimens is longer than that of barrier type anodic oxide specimens. During localized corrosion, the current and potential changing with fluctuations, and the potential and the current fluctuations show good correlation. The slope of the PSD of both potential spectra of anodized specimens is about minus one (-1), after the localized corrosion has started. This technique allows observation of electrochemical impedance changes during localized corrosion.

KEY WORDS

Electrochemical noise, Electrochemical impedance, Anodizing, Aluminum, Galvanic corrosion, Chloride ion

INTRODUCTION

Aluminum and its alloys are widely used because of their high strength-weight ratio and good corrosion resistance. Aluminum and its alloys are sometimes joined to other metals in specific applications; galvanic corrosion may occur in such situations and this is a serious problem for the durability of some systems.

Aluminum and its alloys are usually used after surface treatment processing, such as anodizing. There are two types of anodic oxide films that can be formed on aluminum, a porous type and a barrier type [1-4]. Barrier type anodic oxide film has an amorphous structure [5] and the thickness depends on the anodizing potential or voltage. Porous type anodic oxide film has an outer porous layer and an inner barrier layer [6]. The porous layer thickness increases linearly with anodizing time and the barrier layer thickness is dependent on anodizing solution and current density. Barrier type anodic oxide films are commonly used in electrolytic capacitors, and porous type anodic oxide films are used as insulators to create both 2D and 3D structures [7-10] or molds [11]. However, the extent of the effect of the anodizing surface treatment on the corrosion resistance of aluminum has not been established.

Recently, an electrochemical random signal (electrochemical noise) analysis technique has been applied in a number of corrosion environments [12-18]. Bertocci et al. [12, 13] has reported a electrochemical noise technique combined with FFT (Fast Fourier Transformation) employing a corrosion couple. Sakairi et al. has applied electrochemical random signal analysis to galvanic corrosion of anodized pure aluminum [19]. They reported that the impedance of porous type anodic oxide films were larger than that of barrier type anodic oxide film. Traditional electrochemical impedance, EIS, techniques are not suitable to measure the impedance during galvanic corrosion, but, the electrochemical random signal analysis technique can obtain the impedance even with localized corrosion, because the impedance is calculated using the power spectrum density (PSD) of the current and potential.

The purpose of this study is to apply the new electrochemical random signal analysis technique to galvanic corrosion of anodized aluminum alloys and to examine the effect of the kind of anodic oxide film on galvanic corrosion resistance.

EXPERIMENTAL

Specimen

First, 6061-T6 aluminum alloy sheets (0.1 mm thickness) were cut to 20 x 20 mm with a handle. The specimens were cleaned in ethanol and in doubly distilled water in an ultrasonic bath.

Anodizing

Barrier type anodic oxide films, Type I, were formed by anodizing at 293 K in 0.5 kmol/m^3 H_3BO_4 / 0.05 kmol/m^3 $Na_2B_4O_7$ solution with constant current density, i_a = 10 A/m^2, and then with a constant potential, E_a = 50 V for 1.8 ks. Porous type anodic oxide films, Type II, were formed by anodizing at 263 K in 3.72 kmol/m^3 H_2SO_4 solutions with a constant current density, i_a = 100 A/m^2 for 600 s. After anodizing, specimen edges were sealed by silicon resin and the exposes area was 1 cm^2.

Electrochemical measurements

Specimens were dipped in 0.5 kmol/m^3 H_3BO_4 / 0.05 kmol/m^3 $Na_2B_4O_7$ solution with 0.3 kmol/m^3 NaCl, and connected with a 16 cm^2 Pt plate (artificial cathode) as a counter electrode, to form a galvanic couple. Fig. 1 shows a schematic outline of the experimental setup. The galvanic current between specimen and counter electrode, and the specimen potential during the test were measured by a computer through an A/D converter and electrochemical signals were measured at one second intervals. The records of the current and potential were processed by calculating the power spectrum density

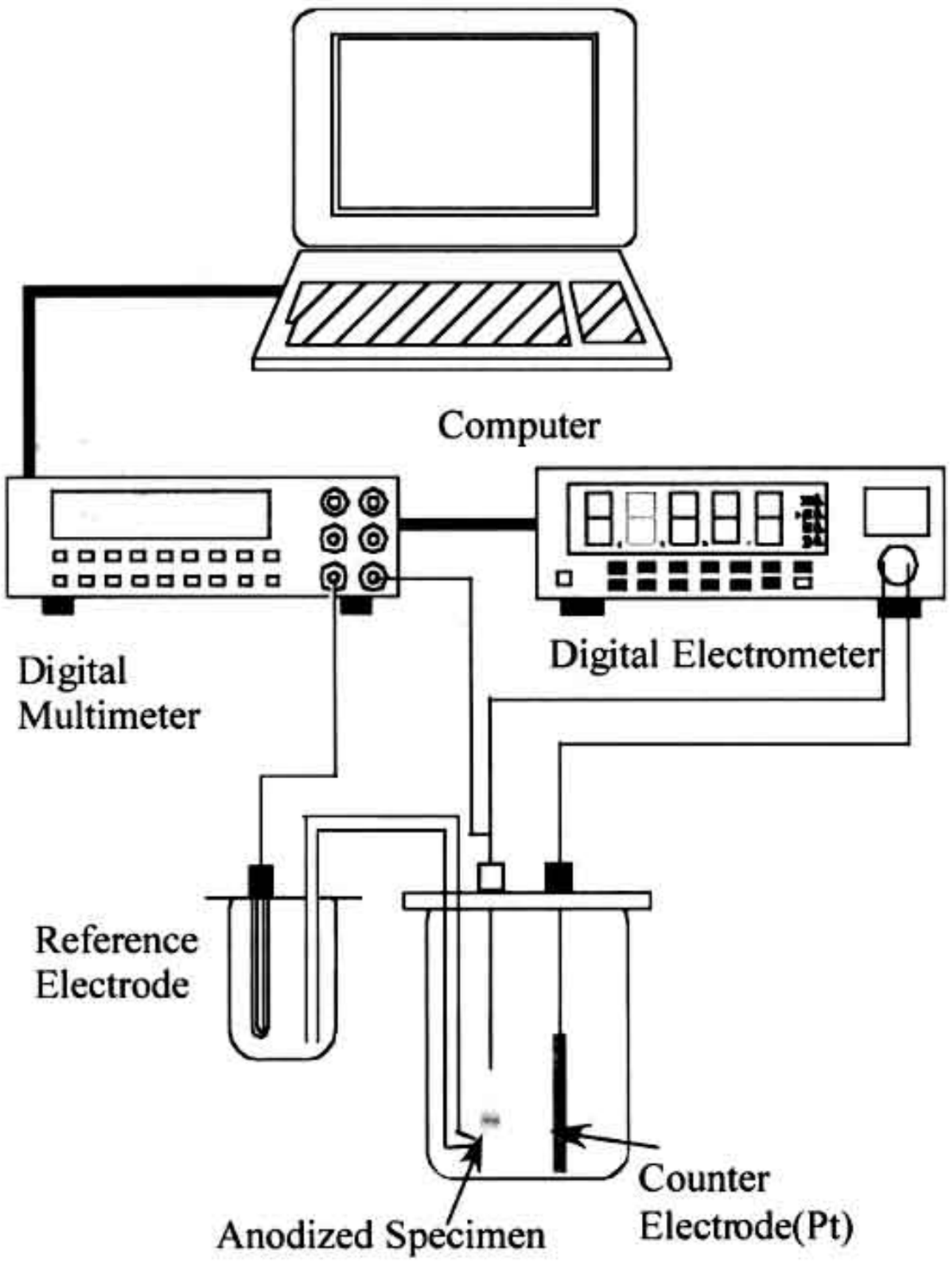

Fig. 1 Schematic outline of the experimental setup.

(PSD) with the FFT method. To calculate PSD, a rectangular window was used. The electrochemical noise impedance was calculated from the current PSD and potential PSD values.

A saturated Ag/AgCl electrode was used as the reference electrode in the measurements of the potential.

Surface observations

The specimen surfaces were examined by confocal scanning laser microscopy (CSLM; Laser Tech. Co. 1SA-21) and scanning electron microscopy (SEM; JEOL, FE-6500F) after the anodizing and the galvanic corrosion tests.

RESULTS AND DISCUSSION

Anodizing behavior

Figure 2 shows the changes in current, i_a, and potential, E_a, with time during anodizing in 0.5 kmol/m^3 H_3BO_4 / 0.05 kmol/m^3 $Na_2B_4O_7$ at 293 K. The potential change of capacitor grade pure aluminum is also shown in the figure. With the 6061 alloy specimen, the potential increases with anodizing time while the current is constant, and after the change to constant potential, the current decreases steeply with time before flattening out to an almost constant value. The slope of the potential, the anodic oxide film growth rate, of the 6061 alloy is one tenth that of aluminum. This may be due to dissolution of alloying elements, such as magnesium and copper, by the high electric field during anodizing. This result suggests that the number of defects

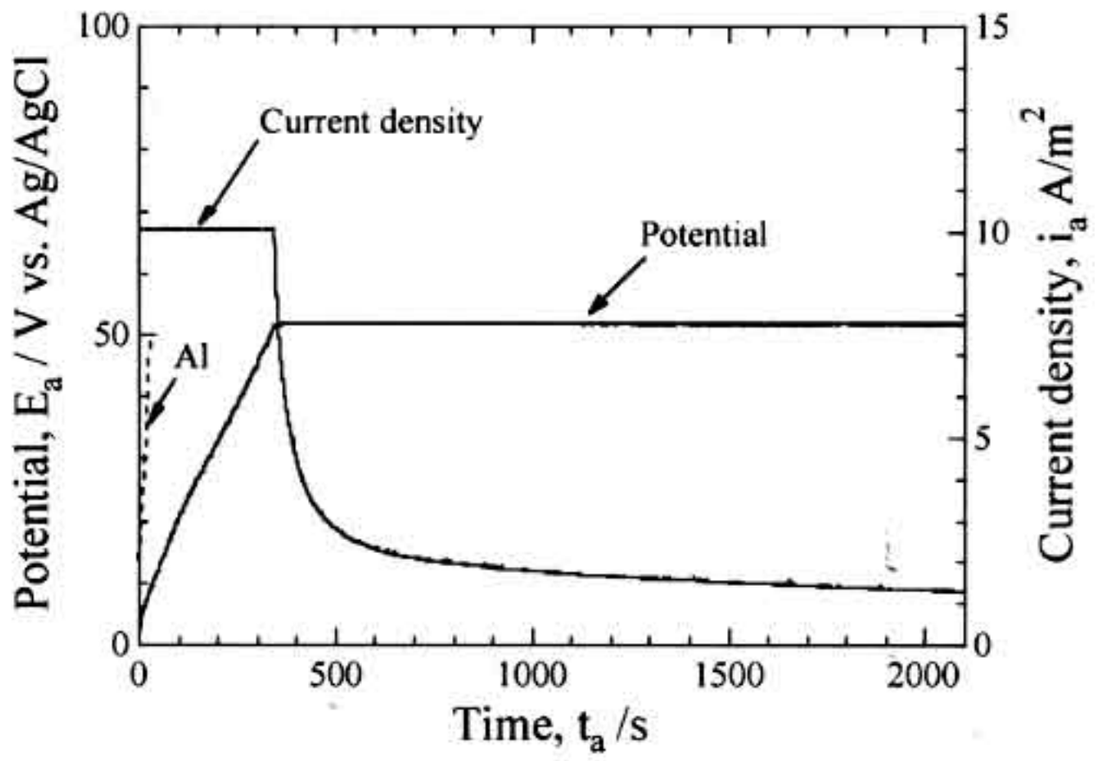

Fig. 2 Changes in current, i_a, and potential, E_a, with time during anodizing in 0.5 kmol/m^3 H_3BO_4 / 0.05 kmol/m^3 $Na_2B_4O_7$ at 293 K.

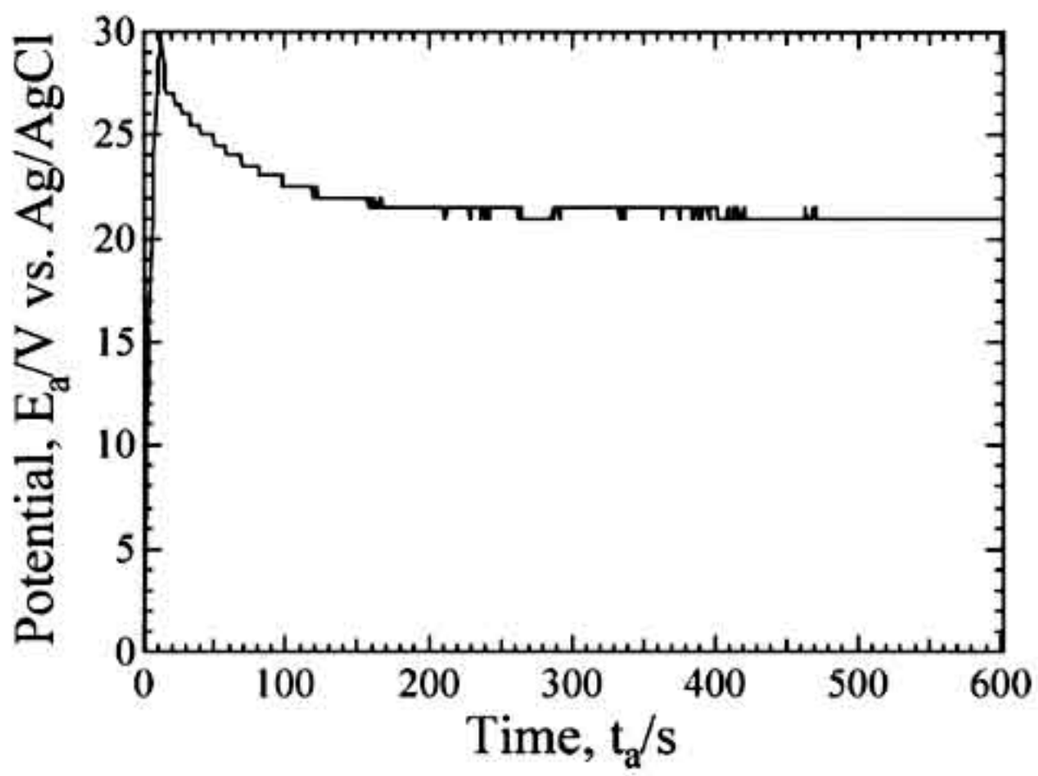

Fig. 3 Changes in potential, E_a, with time during anodizing in 3.72 kmol/m^3 H_2SO_4 at 263 K.

in the film formed on the 6061 alloy may be larger than that formed on the aluminum specimens. However, the result also suggests that the anodic oxide film structure and thickness of the 6061 specimen are very similar to those of aluminum. The anodizing ratio of aluminum anodic oxide film is about 1.5 nm/V. Therefore the estimated oxide film thickness is about 75 nm.

Figure 3 shows the change in potential, E_a, with time during anodizing in 3.72 kmol/m^3 H_2SO_4 at 263 K. The potential increases through a transient region at about 30 V and subsequently deceases to an approximately constant potential of about 22 V. The rate of increase and constant potential of the 6061 alloy were almost the same as those of aluminum. This suggests that the alloying elements do not affect the anodizing behavior in H_2SO_4 solutions. The estimated barrier layer thickness is about 25 nm and the estimated porous layer thickness is about 1.8 μm. Fig. 4 shows a schematic outline of both type I (barrier) and type II (porous) anodic oxide films.

Electrochemical random signal

Figure 5 shows the changes in the potential and current

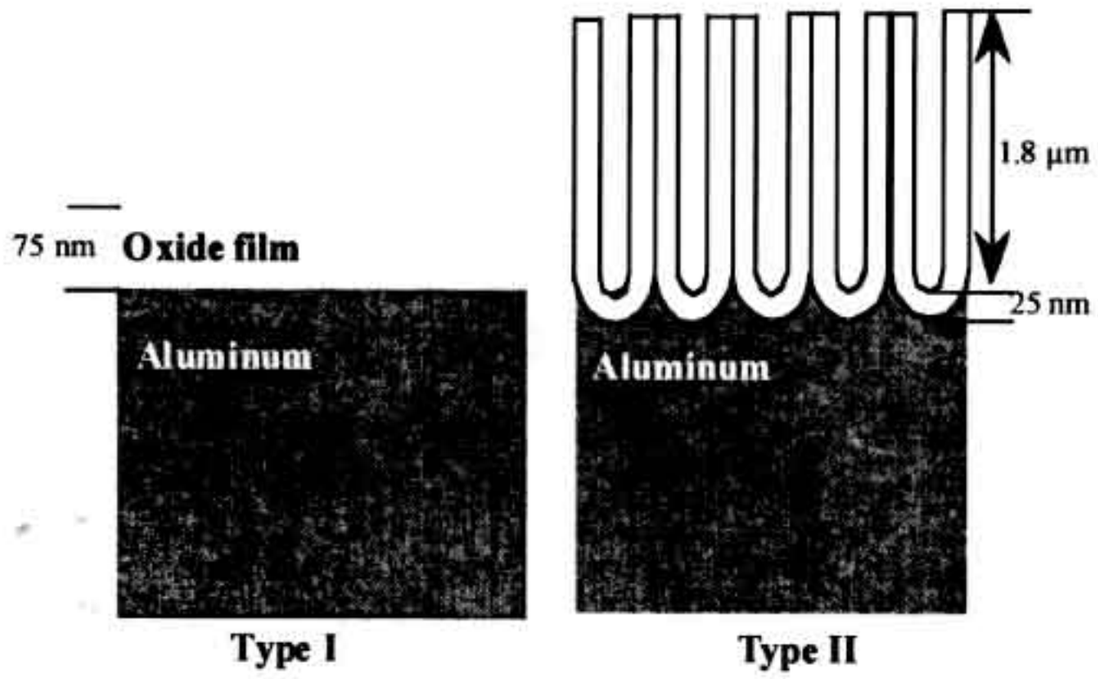

Fig. 4 Schematic outline of the anodic oxide films

with immersion time, t_i, during galvanic corrosion of Pt coupled to 6061 alloy covered with type I anodic oxide film in 0.5kmol/m^3 H_3BO_3 / 0.05 kmol/m^3 $Na_2B_4O_7$ with 0.3 kmol/m^3 NaCl. During the incubation period ($t_i < 5$ s), nether the current nor the potential changes from their initial values, however, after 5 s the potential decreases with immersion time and the current increases through a maximum at about 50 s and subsequently decreases. With longer immersion time, the potential reached a constant value of -800 mV and the current increased again to show almost constant value of 900μA. After the galvanic corrosion test, the specimen surface was covered by corrosion products.

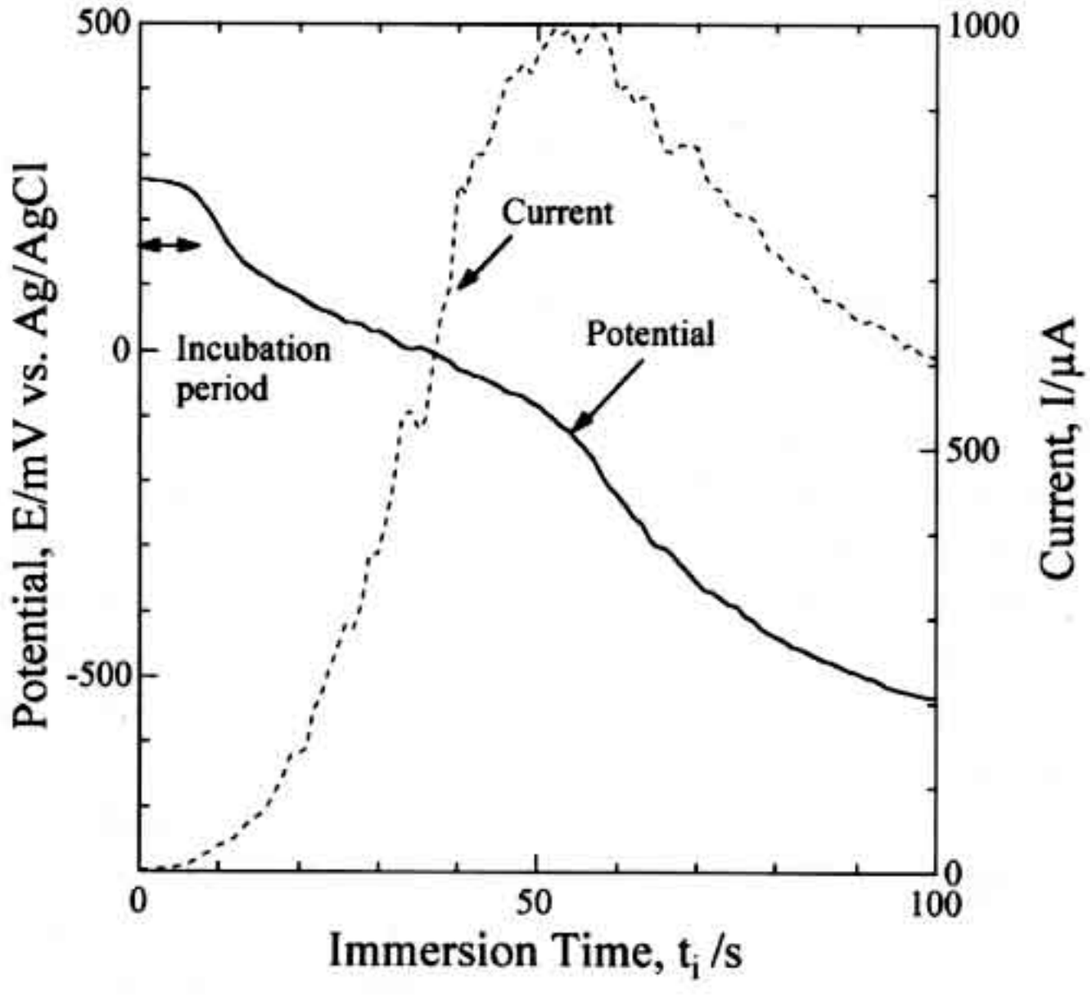

Fig. 5 Changes in the potential, and current with immersion time, t_i, during galvanic corrosion of Pt coupled to 6061 alloy covered with type I anodic (barrier) oxide film in 0.5kmol/m^3 H_3BO_3 / 0.05 kmol/m^3 $Na_2B_4O_7$ with 0.3 kmol/m^3 NaCl.

Figure 6 shows the changes in the potential and current with immersion time during galvanic corrosion of Pt coupled to the 6061 alloy covered with type II anodic oxide film in 0.5kmol/m^3 H_3BO_3 / 0.05 kmol/m^3 $Na_2B_4O_7$ with 0.3 kmol/m^3 NaCl. During the incubation period (< 150 s), neither current nor potential changes from the initial values, however, after 150 s, there are sudden changes as indicated by the electrochemical random signal fluctuations, related to localized corrosion. The incubation period of the type II film specimen is more than ten times longer than that of the type I film specimen. The localized corrosion and pitting corrosion are stochastic phenomena, however this behavior is very similar in all experiments. If only the barrier layer affects the corrosion resistance of the sample, the incubation period of the type I film specimen should be longer than that of the type II film specimen. Because, the barrier layer thickness of the type I film is about three times thicker that of the type II film. This difference in incubation periods indicates that the porous structure is more effective than the barrier layer in improving corrosion resistance.

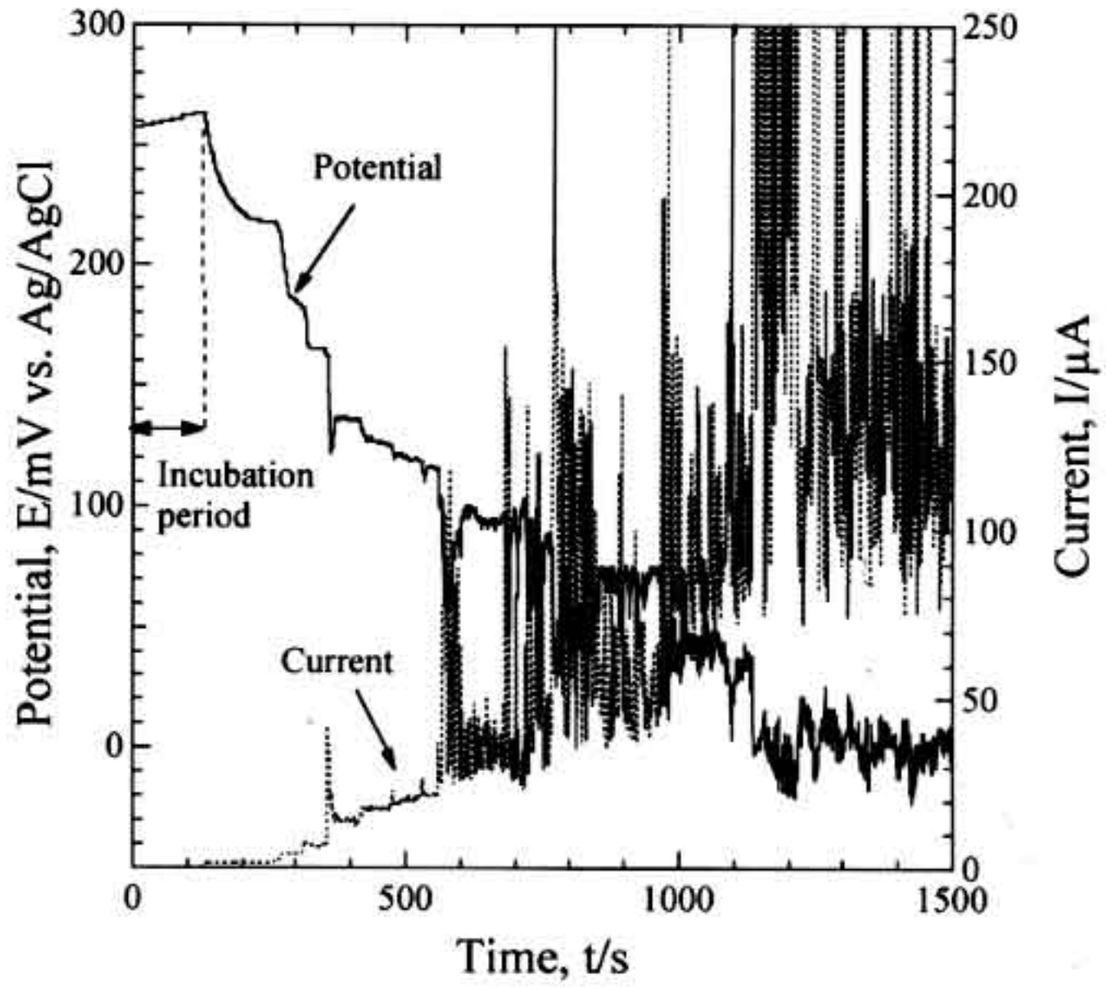

Fig. 6 Changes in the potential and current with immersion time during galvanic corrosion of Pt coupled to 6061 alloy covered with type II (porous) anodic oxide film in 0.5kmol/m^3 H_3BO_3 / 0.05 kmol/m^3 $Na_2B_4O_7$ with 0.3 kmol/m^3 NaCl.

Figure 7 is a magnification of the potential and current in Fig. 6 after the localized corrosion has started, showing that the potential and current move in opposite directions, with good correlation. The current and potential fluctuations may be related to individual events in the generation, growth, and extinction of localized or pitting corrosion. The computed pit size using the current fluctuations suggests pits of several tens μm, when the shape of a pit is hemispherical and aluminum dissolves as Al^{3+}.

Figure 8 is a schematic outline of a) pit growth with elapsed time, b) anodic and cathodic partial current, and c) current and potential transient at a pitting events. During pitting corrosion, the rate of cathodic reaction and anodic reaction do not change, but area of dissolution and the anodic reaction site changes, a). This area expansion causes the increase in the anodic polarization curves, b).

After some time, the alloy surface would be covered by corrosion products and the anodic current returns to the previous value. The measured potential and current during the test are the points where the anodic and cathodic curves cross. Once pitting or localized corrosion starts on the specimen surface, the current and potential are changed over time as in Fig. 8 c).

PSD of electrochemical random signal and impedance

The electrochemical results of the Type I film specimen are not suitable for impedance analysis. This new electrochemical random signal technique can be applied to measure the impedance as the amplitude of potential random signals of about several tens of mV. The electrochemical data in Fig 6 contains the DC component and minus the averages of the trend in the potential and current changes before compute PSD. The DC component and trend of the signal must be subtracted, otherwise PSD has a large error. Figure 9 shows the potential and current random signals selected after the 512 s point in Fig. 6 after the DC component and trend were removed.

Figure 10 shows the PSD of the a) potential and b) current in Fig. 9. The potential and current PSD decrease with increasing frequency, and the slopes are steeper than

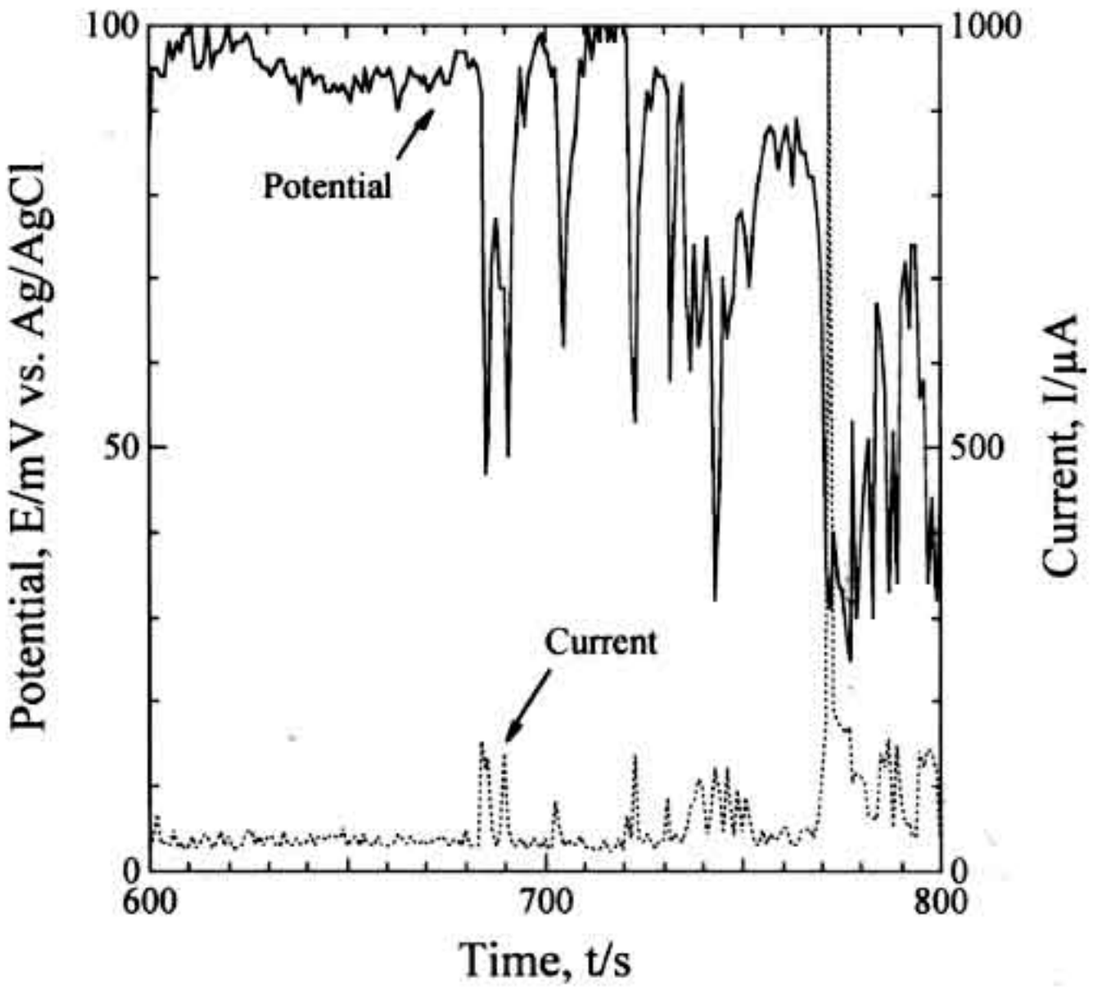

Fig. 7 Magnification of the potential and current in Fig. 6 after the localized corrosion has started.

or equal to -1. A slope -1 indicates that each event, each pitting corrosion event, occurs independent of other events.

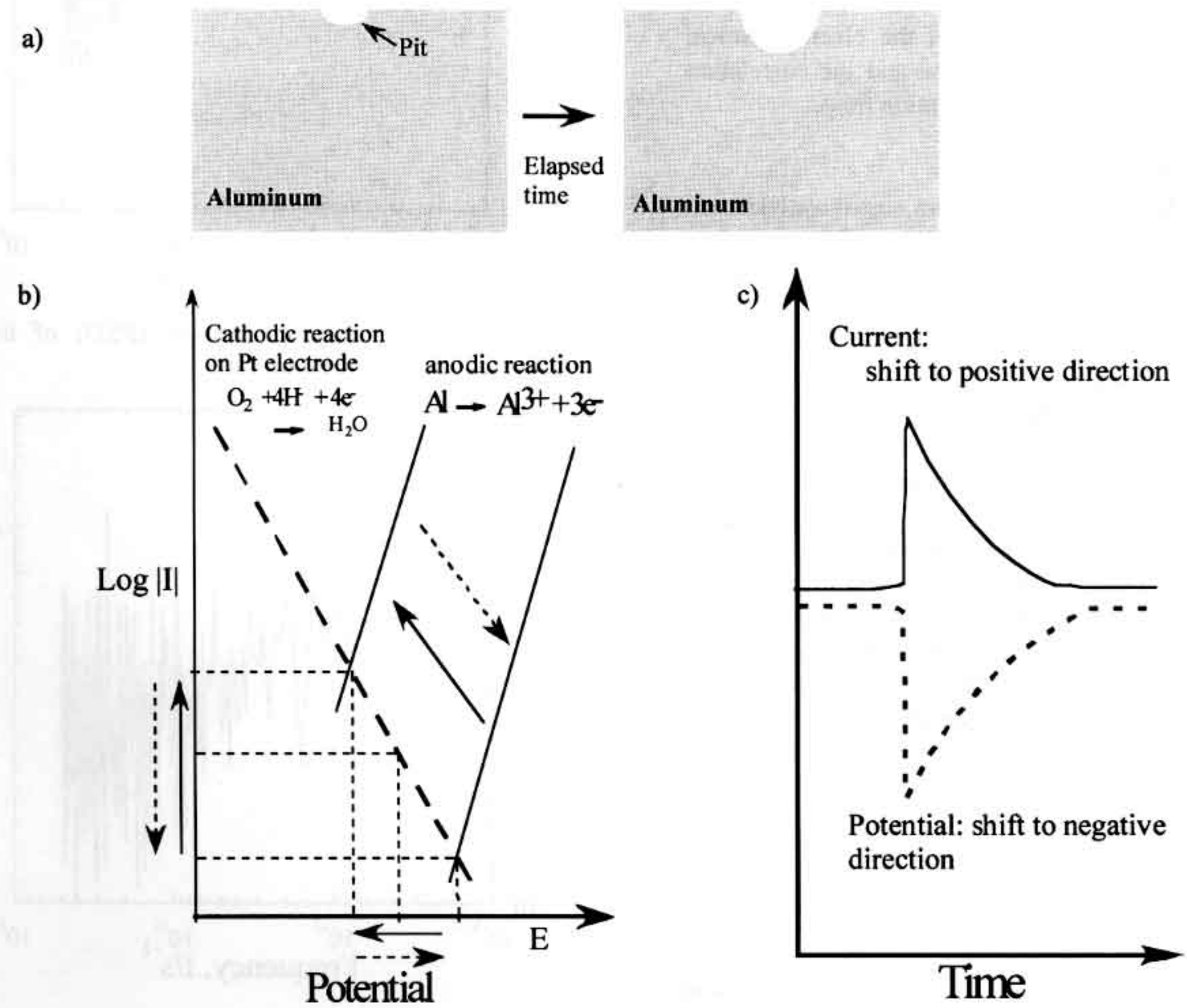

Fig. 8 Schematic representation of a) pit growth, b) polarization curves and c) current, and potential transients.

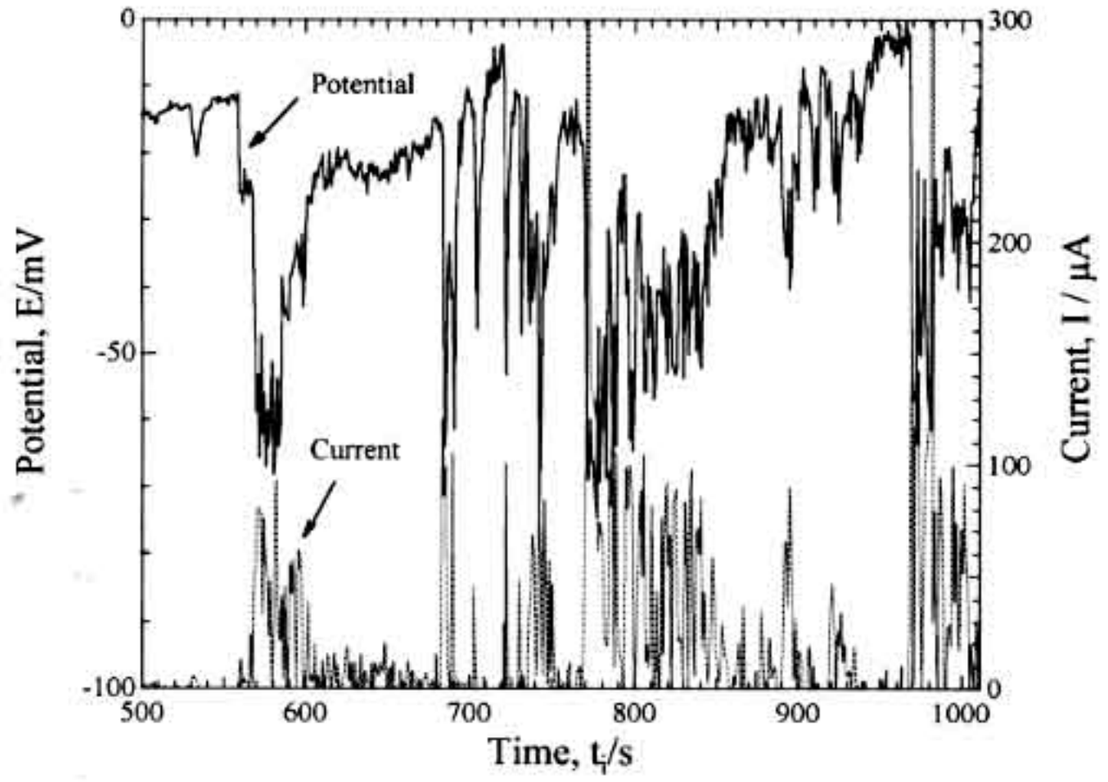

Fig. 9 Potential and current random signal in Fig. 6 after the DC component and trend were removed.

The electrochemical impedance can be computed by using the potential and current PSD.

$$Z(\omega) = \frac{P(\omega)}{I(\omega)}$$

Figure 11 shows the electro chemical impedance spectrum. The impedance decreases slightly with increasing frequency, as the slope of the current PSD is steeper than -1. The mean value of the electrochemical noise impedance decreased with time and the correlation coefficient also decreased with immersion time.

CONCLUSIONS

A new type of electrochemical random signal analysis was applied to galvanic corrosion of aluminum alloy specimens with anodic oxide film. The following conclusions can be drawn:

During the incubation period, the initial current and potential values change only slightly with time. When localized corrosion has started, however, these values change suddenly and continuously with fluctuations. The potential and the current fluctuations show a close correlation.

The slope of the current and potential PSD spectra of the anodized specimens is about minus one (-1) after the localized corrosion has started. The random signal technique employed for makes it possible to measure the electrochemical impedance during localized corrosion and the values do not change with frequency.

Acknowledgements

The authors thank Nippon Keikinzoku Co. for providing the aluminum and its alloy samples.

REFERENCES

[1] K. Watanabe, M. Sakairi, H. Takahashi, S. Hirai, and S. Yamaguchi: Formation of Al-Zr Composite Oxide Films on Aluminum by Sol-Gel Coating and Anodizing, J.

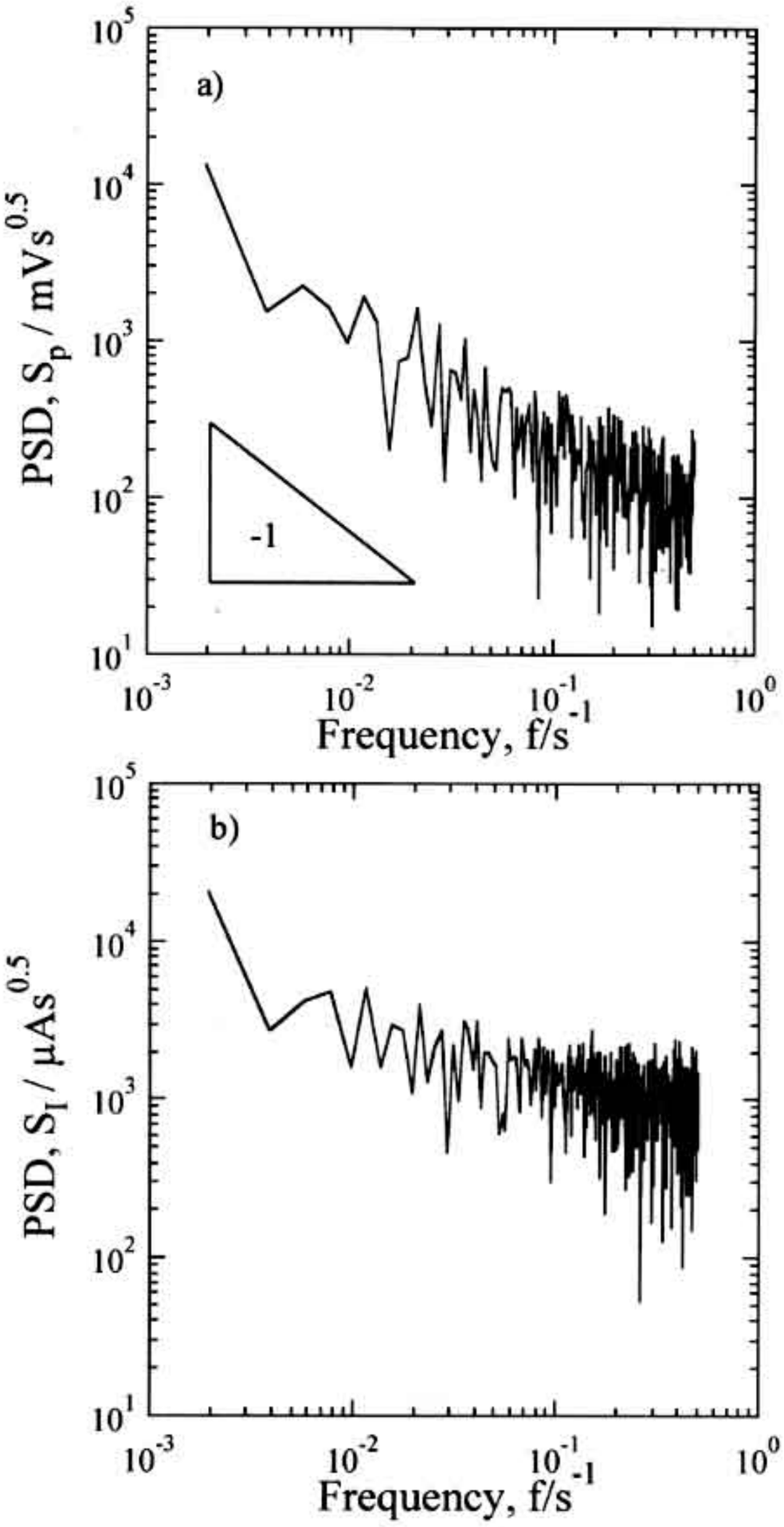

Fig. 10 Power spectrum density (PSD) of the a) potential and b) current in Fig 9

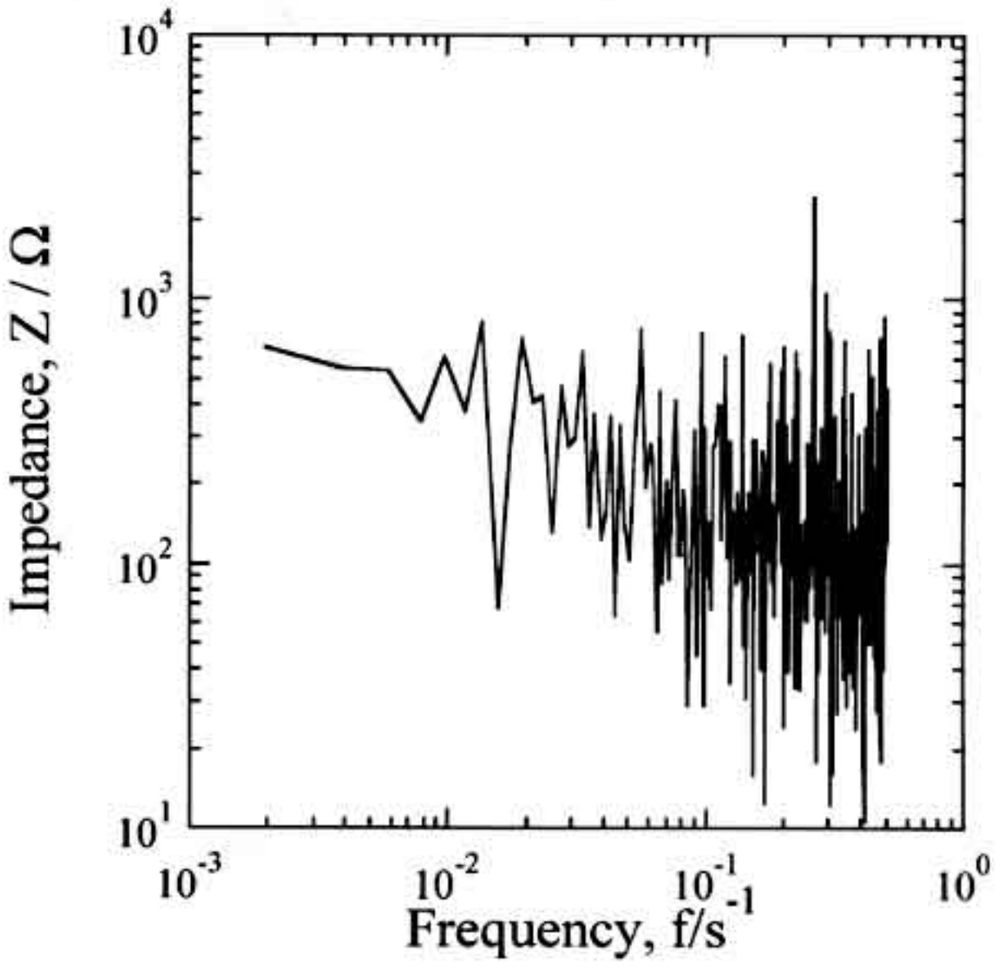

Fig. 11 Impedance of noise data observed on type II anodic specimens.

Electroanal. Chem., 473, (1999) 250-255.
[2] Y. Li, S. Shigyo, M. Sakairi, H. Takahashi and M. Seo: Formation of Al / (Ti, Nb, Ta) - Composite Oxide Films on Aluminum by Pore-FillingJ. Electrochm. Soc., 144 (1997), 866.
[3] M. Sakairi, P. Skeldon, G. E. Thompson, G. C. Wood and K. Stevens: Effect of Current Density During Anodizing of 2024 Aluminum Alloy in Sulfuric Acid at Low Temperature, Proc. of ASST 2000 (2000), 410-415.
[4] M. Sakairi, P. Skeldon, G. E. Thompson, G. C. Wood: Effect of Benzotriazole on Anodizing of 2024 Aluminum Alloy in Sulfuric Acid at Low Temperature, Electrochem. Soc. Proc., 99-27 (1999), 171-180.
[5] Y. Takashima, K. Miwa, M. Sakairi and H. Takahashi: In situ AFM Observation of Growth of Anodic Oxide Films on Aluminum -Mechanism of Flattening of the Film Surface-, J. Surf. Fin. Soc. Jpn., 51 (2000), 625-632.
[6] M. Sakairi, Z. Kato, S. Chu, H. Takahahshi, Y. Abe and N. Katayama: Local Removal of Thick Anodic Oxide Film on Aluminum with A Photon Rupture Technique and Local Metal Deposition, Electrochemistry, 71 (2003), 920-926.
[7] S. Z. Chu, M. Sakairi and H. Takahashi: Copper Electroless Plating at Selected Area on Aluminum with Pulsed Nd-YAG Laser, J. Electrochme. Soc., 147 (2000), 1423-1430.
[8] S. Z. Chu, M. Sakairi and H. Takahashi, K. Shimamura, and Y. Abe: Laser-assisted Electroless Ni-P Deposition at Selected Areas on Al (-Mg, Si, Cu) Alloys, J. Electrochme. Soc., 147 (2000), 2181-2189.
[9] T. Kikuchi, M. Sakairi, H. Takahashi, Y. Abe and N. Katayama: Fabrication of Nickel Micro-Pattern on Insulating Board by Anodizing/Laser Irradiation/ Electrodeposition, Surface and coatings technology, 169-170 (2003), 199-203.
[10] T. Kikuchi, M. Sakairi, H. and Takahashi: Three-dimensional Microstructure Fabrication with Anodizing, Laser Irradiation, and Electrodeposition, J. Electrochem. Soc. 150 (2003), C567-C572.
[11] H. Masuda, F. Matsumoto and K. Nishio: Fabrication of Functional Devices Based on Highly Ordered Anodc Porous Alumina, Electrochemistry, 72 (2004), 389-394.
[12] U. Bertocci, C. Gabrielli, F. Huet and M. Keddam: Noise Resistance Applied to Corrosion Measurements I. Theoretical Analysis, J. Electrochem. Soc., 144 (1997), 31-37.
[13] U. Bertocci, C. Gabrielli, F. Huet M. Keddam and P. Rousseau: Noise Resistance Applied to Corrosion Measurements II. Experimental Tests, J. Electrochem. Soc., 144 (1997), 37-41.
[14] T. Tsuru and M. Yaginuma: Corrosion Rate Estimation Based on Electrochemical Noise Analysis, Zairyo-to-Kankyo, 52 (2003), 488-495.
[15] H. Yashiro, M. Kumagai and N. Kumagai: Analysis of Potential Fluctuation for an Embryonic Stage of SCC Sensitized SUS 304 Stainless Steel in Chloride Solution, Zairyo-to-Kankyo, 52 (2003), 466-470.
[16] Y. Ioti, S. Take and Y. Okuyama: Electrochemical Noise in Crevice Corrosion of Aluminum and Possibility for Its Monitoring, Zairyo-to-Kankyo, 52 (2003), 471-476.
[17] Y. Yoneda and H. Inoue: Potential Noise of Carbon Steel in Deaerated Chloride Solutions Containing Sodium Nitrite, Zairyo-to-Kankyo, 52 (2003), 495.
[18] H. Inoue, M. Kinoshita and Y. Maeda: The Estimation of the Threshold State of Stress Corrosion Cracking Based on the Distribution of the Electricity Quantities of Local Anodic Currents Estimated from Potential Fluctuation -Basic Investigation on the Use of Potential Fluctuation Measurement for SCC Monitoring-, Zairyo-to-Kankyo, 52 (2003) 483-487.
[19] M. Sakairi, Y. Shimoyama and H. Takahashi: Electrochemical Noise Analysis of Galvanic Corrosion of Anodized Aluminum in Chloride Environments Electrochemistry, 74, 458 (2006).